Inorganic Chemistry

Article

pubs.acs.org/IC

Enhanced Catalysis Activity in a Coordinatively Unsaturated Cobalt-MOF Generated via Single-Crystal-to-Single-Crystal Dehydration

Hai-Yun Ren, Ru-Xin Yao, and Xian-Ming Zhang*

School of Chemistry & Material Science, Shanxi Normal University, Linfen 041004, P. R. China

Supporting Information

ABSTRACT: Hydrothermal reaction of $Co(NO_3)_2$ and terphenyl-3,2″,5″,3′-tetracarboxylate (H_4tpta) generated $Co_3(OH)_2$ chains based 3D coordination framework $Co_3(OH)_2$(tpta)$(H_2O)_4$ (**1**) that suffered from single-crystal-to-single-crystal dehydration by heating at 160 °C and was transformed into dehydrated $Co_3(OH)_2$(tpta) (**1a**). During the dehydration course, the local coordination environment of part of the Co atoms was transformed from saturated octahedron to coordinatively unsaturated tetrahedron. Heterogenous catalytic experiments on allylic oxidation of cyclohexene show that dehydrated **1a** has 6 times enhanced catalytic activity than as-synthesized **1** by using *tert*-butyl hydroperoxide (*t*-BuOOH) as oxidant. The activation energy for the oxidation of cylcohexene with **1a** catalyst was 67.3 kJ/mol, far below the value with **1** catalysts, which clearly suggested that coordinatively unsaturated Co^{II} sites in **1a** have played a significant role in decreasing the activation energy. It is interestingly found that heterogeneous catalytic oxidation of cyclohexene in **1a** not only gives the higher conversion of 73.6% but also shows very high selectivity toward 2-cyclohexene-1-one (ca. 64.9%), as evidenced in high turnover numbers (ca. 161) based on the open Co(II) sites of **1a** catalyst. Further experiments with a radical trap indicate a radical chain mechanism. This work demonstrates that creativity of coordinatively unsaturated metal sites in MOFs could significantly enhance heterogeneous catalytic activity and selectivity.

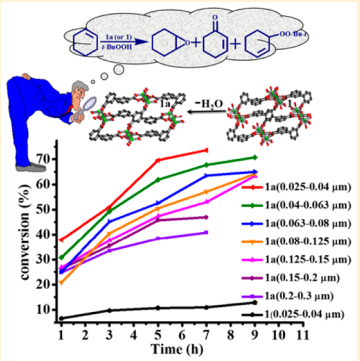

INTRODUCTION

The radical oxidations of cyclic olefin are widely used in the bulk chemical industry as well as the synthesis of value-added fine chemicals.[1] Among these cyclic olefins, oxidation of cyclohexene is especially important since the oxidation products, α,β-unsaturated ketones, are valuable intermediates in the fragrance industry and organic synthesis. Although many studies have revealed that the oxidation of cyclohexene could be selectively catalyzed by homogeneous transition-metal (Fe, Cr, Ru, Mn, Cu, Co, etc.) catalysts,[2] their performance is still limited by the great difficulty in separation and recyclable use. From an environmental and an economic viewpoint, corresponding heterogeneous catalysts are desired to improve the processes by offering numbers of advantages over homogeneous catalysts, including easy separation, efficient recycling, minimizing metal trace in the product, and improved handling and process control.[3] However, it remains very hard for heterogeneous catalysts to explain the catalytic mechanisms because many more complex techniques are needed to study the adsorbed active species on solid surfaces in a heterogeneous catalytic system.

Recently, metal−organic frameworks (MOFs) based heterogeneous catalysts have been attracting the interest of the material scientists because they precede general immobilized catalysts in several important ways, such as high catalyst loadings, more accessible and identifiable catalytic centers, and the more flexible design of structural building units.[4] The catalytically active sites can be implemented at the organic or the inorganic component of frameworks by direct synthesis of the envisaged scaffold or by postsynthetic modification. For example, the metal sites with unsaturated coordination environments can be created via removal of terminal coordinated water or other solvent molecules, which can be utilized as catalytically active sites.[5] However, creation of active sites via external stimuli such as heat or mechanic force will generally produce defects and damaged regions, which prevents at the atomic level characterization of coordinatively unsaturated metal centers via X-ray single-crystal diffraction. Therefore, it is still a challenge to create coordinatively unsaturated metal centers via single-crystal-to-single-crystal (SCSC) transformation.[6]

In the ongoing research of porous catalytic frameworks, cobalt based MOFs attract our attention, since Co(II) atoms could display varied coordination geometries such as octahedral, tetrahedral, square-pyramidal, trigonal-bipyramidal, and square-planar. The flexible and diverse local coordination geometries of cobalt make it easy to engineer coordinatively unsaturated metal centers via SCSC transformation. Activated Co(II)-MOFs were found to catalyze allylic oxidation reactions of cyclohexene with O_2 and/or *t*-BuOOH.[7] However, 2-cyclohexen-1-one, a kind of α,β-unsaturated ketones, only as traces occurs in these oxidation reactions. Recently, Cr-MIL-101 could behave as a heterogeneous catalyst to give main α,β-

Received: March 17, 2015
Published: June 5, 2015

DOI: 10.1021/acs.inorgchem.5b00606
Inorg. Chem. 2015, 54, 6312−6318

Scheme 1. (a) In Situ SCSC Dehydration from 1 to 1a. (b) 1a-Catalyzed Allylic Oxidation of Cyclohexene toward α,β-Unsaturated Ketones

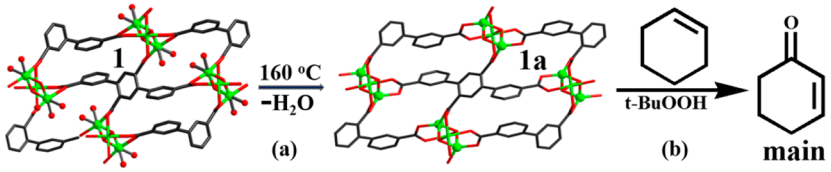

unsaturated ketones in the reactions, but its conversion only achieved 16%.[8] Additionally, little information is available about the specific structures of coordinatively unsaturated metal centers as active sites in these works,[7−9] which made their oxidation mechanisms feeble and futile.

In this Article, by in situ high-temperature SCSC dehydration, $Co_3(OH)_2(tpta)(H_2O)_4$ (**1**) was transformed into $Co_3(OH)_2(tpta)$ (**1a**), during which the local coordination environment of part of the Co atoms was changed from octahedron to coordinatively unsaturated tetrahedron (Scheme 1a). Particular attention is given to investigation into the effect of open Co^{II} sites on the catalytic activity. We found the **1a** exhibits an excellent activity in the allylic oxidation of cyclohexene using *tert*-butylhydroperoxide (*t*-BuOOH) as oxidant and selectively catalyzes the oxidation reaction toward formation of *α,β*-unsaturated ketone (Scheme 1b). The higher catalytic activity and selectivity are rare, if not unique, in the field. Furthermore, by the calculation of activation energy and radical trap experiments, we proposed a plausible mechanism to rationalize the high catalytic activation and selectivity for the **1a** catalytic oxidation.

EXPERIMENTAL SECTION

Materials and Methods. All chemicals were analytically pure from commercial sources and used without further purification, unless otherwise noted. 1,2,4-Trichlorobenzene was chromatographically pure. Cyclohexane and cyclohexene were dried with anhydrous $CaCl_2$. *t*-BuOOH was dried with anhydrous $MgSO_4$ in an ice bath. Elemental analyses were performed on a Vario EL-II analyzer. FTIR spectra were recorded from KBr pellets in the range of 4000−400 cm^{-1} on a PerkinElmer Spectrum BX FT-IR spectrometer. Variable-temperature powder X-ray diffraction (VTPXRD) and powder X-ray diffraction (PXRD) data were collected in a Bruker D8 advance diffractometer. The purity of all compounds was confirmed by comparison of experimental PXRD patterns with the simulated pattern derived from the X-ray single-crystal data compound. The thermogravimetric analyses (TGA) were carried out in an air atmosphere using SETARAM LABSYS equipment at a heating rate of 10 °C/min. N_2 adsorption measurement was performed using a Micromeritics ASAP 2020HD88 surface area and pore size analyzer, which was conducted up to a relative pressure (p/p_0) of 1.0 on **1a** at STP. UV−vis absorption spectra were recorded on a Cary 5000 (VARIAN) UV−vis−NIR spectrophotometer in a cell with a 1 mm width. GC analysis was performed using an AGILENT 7820 gas chromatograph with a flame ionization detector (FID) and a cross-linked (95%)-dimethyl-(5%)-diphenylpolysiloxane (HP-5) capillary column of 30 m in length. GC/MS analysis was performed using a Thermo Fisher Polaris Q (Ion Trap) gas chromatograph/mass spectrometer and a cross-linked (95%)-dimethyl-(5%)-diphenylpolysiloxane (DB-5) capillary column of 30 m in length. Atomic absorption spectroscopy (AAS) was performed on a Thermo S2 atomic absorption spectrometer.

Syntheses. $Co_3(OH)_2(tpta)(H_2O)_4$ (**1**). A mixture of $Co(NO_3)_2$ (0.116 g, 0.40 mmol), H_4tpta (0.042 g, 0.10 mmol), $HClO_4$ (0.15 mL/3 M, 0.45 mmol), DMF (3 mL), and H_2O (4 mL) was stirred and then sealed in a 15 mL Teflon-lined stainless autoclave at 150 °C for 4 days. After it was cooled to room temperature and subjected to filtration, pink pillar crystals of **1** in a yield of 78.6% (based on H_4tpta) were recovered. Anal. Calcd (%) for $C_{22}H_{20}Co_3O_{14}$ (1): C, 38.56; H, 2.94. Found: C, 38.35; H, 2.83. IR data (KBr, cm^{-1}): 3566(s), 2960(b), 1584(s), 1410(s), 1150(w), 774(s), 586(s).

$Co_3(OH)_2(tpta)$ (**1a**). Complex **1a** was obtained by heating the crystal sample of **1** at 160 °C. Anal. Calcd for $C_{22}H_{10}Co_3O_{10}$ (**1a**): C, 43.24; H, 1.65. Found: C, 43.30; H, 1.68. IR (KBr, cm^{-1}): 3608(w), 3563(s), 2989(w), 1591(s), 1396(s), 1266(w), 773(s), 590(m).

X-ray Crystallography. X-ray single-crystal diffraction data for **1** at 298(2) K and high-temperature X-ray single-crystal diffraction data for **1a** at 458(2) K under a N_2 atmosphere were collected on an Agilent Technologies Gemini EOS diffractometer using Mo K*α* radiation (*λ* = 0.71073 Å). The program SAINT was used for integration of the diffraction profiles, and the program SADABS was used for absorption correction. All the structures were solved by direct methods using the SHELXS program of the SHELXTL package and refined by a full-matrix least-squares technique with SHELXL.[10] All nonhydrogen atoms were refined with anisotropic thermal parameters. Hydrogen atoms of the organic ligand were generated theoretically onto the specific carbon and refined isotropically with fixed thermal factors. Further details for structural analysis are summarized in Table 1, and selected bond lengths and angles are shown in Table S1 of the Supporting Information.

Catalytic Oxidation of Cyclohexene. **1** and **1a** were added to a solution of cyclohexene (3.8 mmol), *t*-BuOOH (14 mmol), and 1,2,4-trichlorobenzene (1 mmol; internal standard) at RT. The reaction mixture was stirred at 70 °C. Aliquots of the reaction mixture (about 0.1 mL) were removed after time intervals indicated in the main text. Each sample was diluted with cyclohexane (1 mL) and filtered through

Table 1. Crystallographic Data and Structure Refinement for 1 and 1a

	1	1a
formula	$C_{22}H_{20}Co_3O_{14}$	$C_{22}H_{10}Co_3O_{10}$
fw	685.17	611.09
crystal system	monoclinic	monoclinic
space group	$P2_1/c$	$P2_1/c$
a (Å)	10.8471(5)	10.769(3)
b (Å)	6.3389(3)	5.8370(19)
c (Å)	16.8839(8)	17.706(5)
α (deg)	90	90
β (deg)	105.592(5)	102.14(3)
γ (deg)	90	90
V (Å^3)	1118.20(9)	1088.0(6)
Z	4	4
ρ_{calc} (g cm^{-3})	2.035	1.865
F(000)	690	606
reflections	4443/2278	4195/2000
data/parameters	2278/184	2000/155
S	1.052	1.068
R_1[a]	0.0573	0.0790
wR_2[b]	0.1549	0.1548
$\Delta\rho_{max}/\Delta\rho_{min}$ (e A^{-3})	1.211/−1.408	1.019/−0.636

[a] $R_1 = \sum||F_o| - |F_c||/\sum|F_o|$. [b] $wR_2 = [\sum[w(F_o^2 - F_c^2)^2]/\sum[w(F_o^2)^2]]^{1/2}$.

DOI: 10.1021/acs.inorgchem.5b00606
Inorg. Chem. 2015, 54, 6312−6318

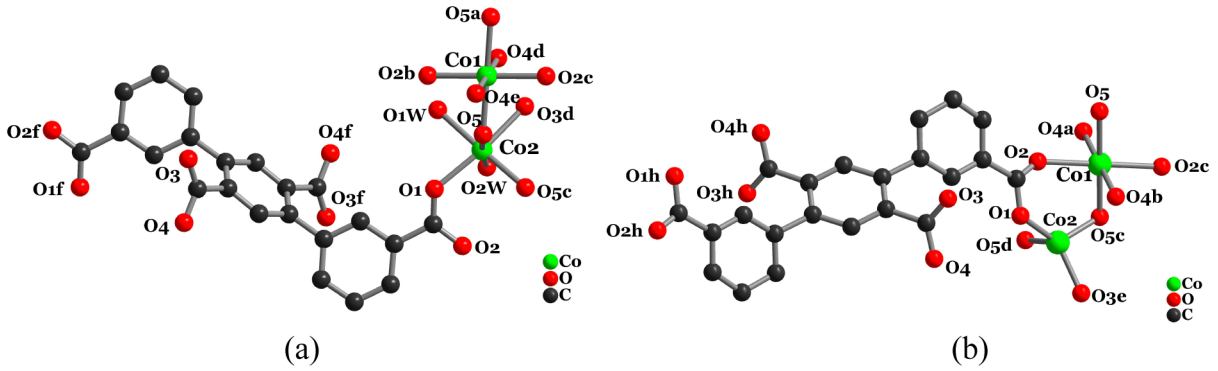

Figure 1. Views of the coordination environments of CoII atoms in **1** (a) and **1a** (b); hydrogen atoms have been omitted for clarity. (Symmetry codes: Compound **1** (a) $-x + 2, -y + 2, -z + 1$; (b) $x, y + 1, z$; (c) $-x + 2, -y + 1, -z + 1$; (d) $x + 1, -y + 3/2, z + 1/2$; (e) $-x + 1, y + 1/2, -z + 1/2$; (f) $-x + 1, -y + 1, -z$. Compound **1a** (a) $x, -y + 3/2, z - 1/2$; (b) $-x, y - 1/2, -z + 1/2$; (c) $-x, -y + 1, -z$; (d) $x, y + 1, z$; (e) $-x, y + 1/2, -z + 1/2$; (f) $-x, -y + 2, -z$; (g) $x, y - 1, z$; (h) $-x + 1, -y + 2, -z + 1$.

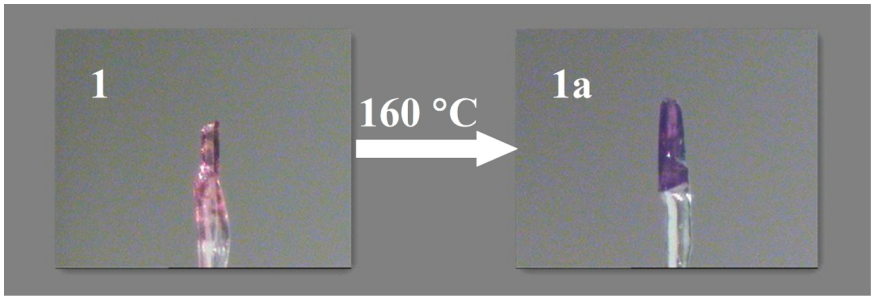

Figure 2. A color change in SCSC dehydration from **1** to **1a**.

a 0.25 mm Acrodisc nylon filter. Then, the sample was identified by GC–MS and quantified by GC. To investigate the influence of crystal size on reaction conversion and yield, polycrystalline samples were ground and sieved into the following particle size ranges: 0.2–0.3, 0.15–0.2, 0.125–0.15, 0.08–0.125, 0.063–0.08, 0.04–0.063, and 0.025–0.04 μm. Since catalytic activity was known to be strongly dependent on the surface area of the catalyst, the curves of conversion and yield as a function of particle size from the measurements made on ground crystals for **1a** are shown in Figures S7 and S8 (Supporting Information). Different amounts of **1a** were reacted with cyclohexene (3.8 mmol) and *t*-BuOOH (14 mmol). For investigations on metal leaching from the catalyst, the hot reaction mixture was filtered at the reaction temperature after 3 h in the case of **1a**. To investigate catalyst activities in subsequent multiple runs, the catalysts were separated from the reaction mixture by centrifugation and rinsed five times with cyclohexane before reuse. All yields and conversions were based on cyclohexene.

RESULTS AND DISCUSSIONS

Description of Structures. Single-crystal X-ray diffraction analysis reveals that compound **1** is a 3D neutral framework based on 1D zigzag chains $Co_3(OH)_2$. Compound **1** crystallizes in the monoclinic space group $P2_1/c$ with an asymmetric unit consisting of two crystallographically independent Co^{II} ions, half $tpta^{4-}$, one hydroxyl, and two coordinated water molecules in Figure 1. The Co1 localizes special positions with a site occupancy of 0.5. The dihedral angle of the two phenyls of $tpta^{4-}$ is 121.2°, in agreement with the semirigid nature of $tpta^{4-}$. The Co1 site adopts an octahedral geometry, coordinated by four carboxylate oxygen atoms (O2b, O2c, O 4d, O4e) in the equatorial plane and two μ_3-OH groups (O5, O5a) in the axial position. The Co1–O distances are in the range of 2.054(3)–2.074(4) Å. The *cis* O–Co1–O angles are in the range of 84.15(14)–95.85(14)°, and the *trans* O–Co1–O angles are 180.000(1)°. The Co2 site also adopts a distorted octahedral geometry, coordinated by two hydroxides (O5, O5c), two carboxylate oxygen atoms (O1, O3d), and two coordinated water molecules (O1w, O2w). The Co2–O distances are in the range of 2.055(4)–2.184(3) Å. The *cis* and *trans* O–Co2–O angles are in the range of 81.25(14)–97.02(15)° and 168.48(16)–176.47(15)°, respectively. The Co^{II} ions are bridged by μ_3-OH groups to form a zigzag $Co_3(OH)_2$ ladder, in which three adjacent Co^{II} ions are arranged into an approximate isosceles triangle. Each isosceles triangle consists of a symmetrically related pair of Co2 atoms (Co2 and Co2c) and a Co1 atom with Co···Co distances of 3.118(2), 3.5145(6), and 3.5494(6) Å. The Co2–O–Co2c, Co1–O–Co2, and Co1–O–Co2c angles are 98.62(15), 117.54(18), and 119.50(18)°, respectively. As observed and confirmed in the cobalt hydroxyl derivatives,[10] the Co2 atoms sharing two μ_3-OH groups are related by ferromagnetic interaction, while antiferromagnetic exchanges might occur between Co1 and Co2 and Co1 and Co2c. As shown in Figure S1 (Supporting Information), **1** adopts a new 4-connected binodal net. The $Co_3(OH)_2$ chains as a zigzag ladder are linked by $tpta^{4-}$ groups which act as 4-connected nodes to furnish the 3D framework with a Schläfli symbol $[4^2.6^3.8]^4[6^2.8^4]$.

In Situ SCSC Transformation. Thermogravimetric analysis (TGA), in situ variable-temperature powder X-ray diffraction (VTPXRD) studies, and in situ high-temperature single-crystal X-ray in the single crystalline phase were all carried out to investigate the SCSC transformations induced by removel of coordinated water molecules in **1**. As shown in Figure S4 (Supporting Information), the VTPXRD differences for **1** recorded in the temperature range of 25–260 °C suggest that coordinated water molecules might be removed around 150–

DOI: 10.1021/acs.inorgchem.5b00606
Inorg. Chem. 2015, 54, 6312–6318

160 °C, which is well documented by the TGA of the first weight loss of 10.2% (calcd 10.6% for two water molecules) in the temperature range of 155−220 °C (Figure S5, Supporting Information). Then, a crystal of **1** was in situ heated to 160 °C to obtain the dehydrated single crystals of $Co_3(OH)_2(tpta)$ (**1a**), which is accompanied by a color change from pink to dark violet (Figure 2). In situ high-temperature single-crystal X-ray diffraction analysis of **1a** shows that the 3D framework remains intact upon dehydration. Compared with **1**, the Co1 atom of **1a** shows a squeezed octahedral geometry, in which the equatorial Co1−O (O1, O1c, O5, O5c) bond lengths slightly stretch about 0.130 Å, and the axial Co1−O (O1, O1c) bond lengths are contracted by around 0.172 Å. The greatest difference in metal coordination environments is that the octahedral environment of Co2 in **1** has been changed into a tetrahedron in the dehydrated phase **1a**; the average Co2−O length in dehydrated **1a** is contracted by 0.117 Å. The changes in the O−Co1−O and O−Co2−O angles are limited to 5.53° and 38.68°, respectively. Compared to the zigzag $Co_3(OH)_2$ ladder in **1**, the average Co···Co distances in **1a** are contracted 0.300 Å, and the changes in Co−O−Co angles are limited to 21.70°. However, the unit cell contains no residual solvent accessible void revealed by PLANTON.[12] The lack of pores can be also confirmed by the negligible N_2 adsorption at cryogenic temperatures (Figure S3, Supporting Information).

UV−Visible Spectra. Electronic spectra of phase-pure microcrystal samples of **1** and **1a** are shown in Figure 3. The

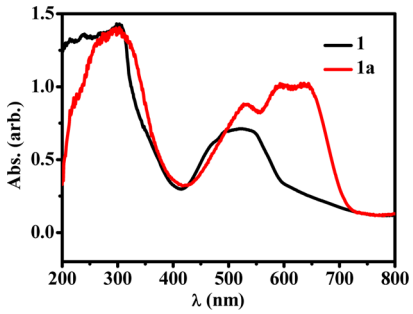

Figure 3. Solid UV−visible spectra of **1** and **1a**.

pink color of compound **1** is consistent with an octahedral environment of divalent cobalt. Compound **1** shows two broad absorption bands. One centered at 256 nm can be assigned to n → π^* transitions, which may be mainly ligand-centered electronic transitions; the other at 519 nm might be ascribed to $[^4T_{1g}(F) \rightarrow {}^4T_{1g}(P)]$ transitions, which are typical of high-spin hexacoordinated octahedral Co^{II} species, being well in accord with the coordination environment of Co atoms in **1**.[13] Compared with **1**, the absorption bands corresponding to n → π^* transitions for the dehydrated phase **1a** are red-shifted to 303 nm. The absorption bands at 530 nm might be ascribed to $[^4T_{1g}(F) \rightarrow {}^4T_{1g}(P)]$ transitions, corresponding to Co1 in octahedral coordination. The dual absorption peaks at 636 nm $[^4A_2 \rightarrow {}^4T_1]$ and 596 nm $[^4A_2 \rightarrow {}^4T_2]$ might be due to Co2 in the tetrahedral coordination geometry, in good agreement with the literatures that the tetrahedron-containing cobalt compounds exhibit typical peaks at lower energies.[14]

Catalytic Allylic Oxidations of Cyclohexene with 1a as Catalyst. Herein, the liquid-phase oxidation of cyclohexene was employed as a test reaction in the screening of catalytic activity parameters over powder **1a**. The reaction was first tested on the oxidation reaction using *t*-BuOOH as oxidant in cyclohexane (10 mL) at 70 °C, giving a conversion (ca. 29.8%) of the oxidant product in 24 h (Figure S6a, Supporting Information). Recently, most reports about the catalytic oxidation of cyclohexene by transition-metal Co^{II} complexes display high selectivity toward formation of *tert*-butyl-2-cyclohexenyl-1-peroxide.[7a,c,15] It is very interesting that **1a** exhibits a higher selectivity toward formation of 2-cyclohexene-1-one (ca. 66.5%) in 12 h (Figure S6b, Supporting Information). A further increase of reaction time to 24 h did not bring about higher conversion and more excellent selectivity. Absence of an accessible void in the unit cell suggests that the open Co(II) sites on the surfaces should be responsible for catalytic activity. To investigate the effects of the particle size of **1a** on conversion and selectivity, different particle sizes of **1a** were employed in the reaction (Figures S7 and S8, Supporting Information, and Table 2). When the reaction was carried out using the particle size of 0.025−0.04 μm of **1a** as catalyst, a higher conversion (ca. 73.6%) was obtained. More intriguingly, the selectivity toward formation of cyclohexenone was still up to 64.9% in 7 h. The TON was as high as about ca.161 (entry 8). These results could be attributed to increasing the surface area of **1a** with more catalytic Co^{II} sites. To further prove the positive effects exerted by open Co^{II} sites, **1** (0.096 mmol) in the same size (0.025−0.04 μm) was tested under the same reaction conditions as well; 12.9% conversion of the oxidation reaction was obtained (Figure S9, Supporting Information), which is probably due to a trace of open Co^{II} sites by grinding. However, much higher conversion was not observed with increased mass of **1a**.

Heterogeneous Nature and Recyclability. To confirm the heterogeneous nature of the catalytic reaction, **1a** was removed from the hot solution by filtration after reaching approximately 50% conversion (which took about 3 h for **1a**). It is clear from Figure 4 that no further catalytic conversion was observed, indicating that cobalt ions (if any) leaching from **1a** are not responsible for the observed activity. The filtrate was also analyzed by atomic absorption spectroscopy (AAS), which indicated that no free cobalt(II) ions in the filtrate were detected due to the concentration of cobalt(II) ions beyond the lower detection limit of the AAS instrument. The results indicated that **1a** behaves as a truly heterogeneous catalyst. The **1a** catalyst can be easily recovered and reused in the oxidation three times with negligible loss of efficiency (see Figure S10, Supporting Information), which indicated reusable and efficiently catalytic activity of **1a**. The crystalline structure of **1a** catalyst was mostly retained after three catalytic cycles (Figure S4, Supporting Information). The higher stability toward degradation during the catalytic process correlates with its higher thermal stability up to 260 °C.

Calculation of Catalytic Activity. As shown in Figure 5, the rate constant (k) for these reactions was determined at different temperatures (50, 60, 70, and 90 °C), which was used to calculate the energy of activation. According to the Arrhenius equation

$$k = Ae^{-(E_a/RT)} \tag{1}$$

After the logarithm, the whole of eq 1 becomes

$$\ln k = \ln A - \frac{E_a}{RT} \tag{2}$$

where R is the gas constant; T, the absolute temperature; A, the preexponential factor; and E_a, activation energy. The plot of ln

DOI: 10.1021/acs.inorgchem.5b00606
Inorg. Chem. 2015, 54, 6312−6318

Table 2. Allylic Oxidation of Cyclohexene with 1a as Catalyst

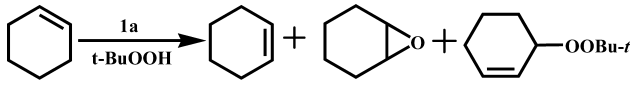

Entry	Particle-size (μm)	Time (h)	Cat (mmol)	Con (%)	Selectivity (%) for 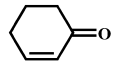		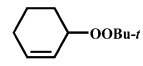	TON[c]
1	Without grinding[a]	24	0.070	29.8	66.5	31.1	2.4	88
2	0.2-0.3[b]	7	0.096	40.8	63.6	28.0	8.4	89
3	0.15-0.2[b]	7	0.096	46.9	51.4	33.2	15.3	102
4	0.125-0.15[b]	7	0.096	52.9	59.0	29.7	11.3	116
5	0.08-0.125[b]	7	0.096	57.1	57.5	26.5	16.0	125
6	0.063-0.08[b]	7	0.096	63.5	67.2	21.4	11.4	139
7	0.040-0.063[b]	7	0.096	67.7	59.3	19.1	21.6	148
8	0.025-0.040[b]	7	0.096	73.6	64.9	22.1	12.9	161

[a]Reaction conditions: cyclohexene (3.8 mmol), *t*-BuOOH (14 mmol), 1,2,4-trichlorobenzene (1 mmol; as internal standard), **1a** (based on cobalt), temp = 70 °C, cyclohexane (10 mL). [b]Solvent-free. [c]TON(turnover number) = moles converted/mol of active Co2 site.

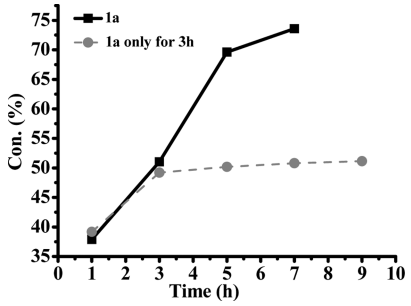

Figure 4. Allylic oxidation of cyclohexene with **1a** as catalyst (black) and filtration of **1a** (gray).

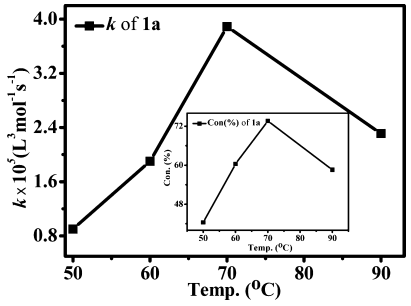

Figure 5. Rate constant (k) vs temperature (°C) curves for the allylic oxidation of cyclohexene with **1a** as catalyst (Inset: conversion (%) vs temperature (°C) curves for the allylic oxidation of cyclohexene with **1a** as catalyst).

k versus T^{-1} gave an activation energy (E_a) in units of kJ·mol^{-1} (Figures S11 and S12, Supporting Information).

As shown in Figure 5 (inset), the conversion in the presence of **1a** increased with the reaction temperature from 50 to 70 °C, but decreased beyond 70 °C, which may be due to the decomposition of *t*-BuOOH without oxidizing cyclohexene. The rate constant (k) for the oxidation of cyclohexene with **1a** catalyst was increased until 70 °C, but on further increasing the temperature beyond 70 °C, the rate constant was decreased (Figure 5). The initial increase in rate constant (k) for the conversion of cyclohexene was an indication that the oxidation of cyclohexene was an energy-activated process. The energy of activation for the oxidation of cylcohexene in the presence of **1a** was 67.3 kJ/mol, far below the value with **1** as catalysts (129.6 kJ/mol) (Table 3), which are well documented that **1a** catalysts played a significant role in decreasing the energy of activation.

Oxidation Mechanism with 1a Catalyst. The radical nature of the oxidation of cyclohexene (**1a** as catalyst) has been confirmed by radical trap experiments. As shown in Table S2 (Supporting Information), the addition of radical scavengers, 2,4,6-tris-*tert*-butylphenole (TTBP) and 2,2,6,6-tetramethylpiperidine-1-oxyl (TEMPO), dramatically suppressed the for-

Table 3. Conversion and Kinetic Parameters at Optimum Molar Ratio of the Allylic Oxidation of Cyclohexene with 1a and 1 as Catalyst, Respectively

catalysts	temp. (°C)	con (wt %)	k (mol^{-1}·L^3·s^{-1})	E_a (kJ/mol)
1a	50	42.4	9.01×10^{-7}	67.3
	60	60.4	1.90×10^{-6}	
	70	73.6	3.89×10^{-6}	
1	50	4.8	1.54×10^{-8}	129.6
	60	8.2	6.23×10^{-8}	
	70	12.9	2.34×10^{-7}	

DOI: 10.1021/acs.inorgchem.5b00606
Inorg. Chem. 2015, 54, 6312−6318

Scheme 2. Proposed Reaction Pathways of the 1a-Catalyzed Allylic Oxidation of Cyclohexene

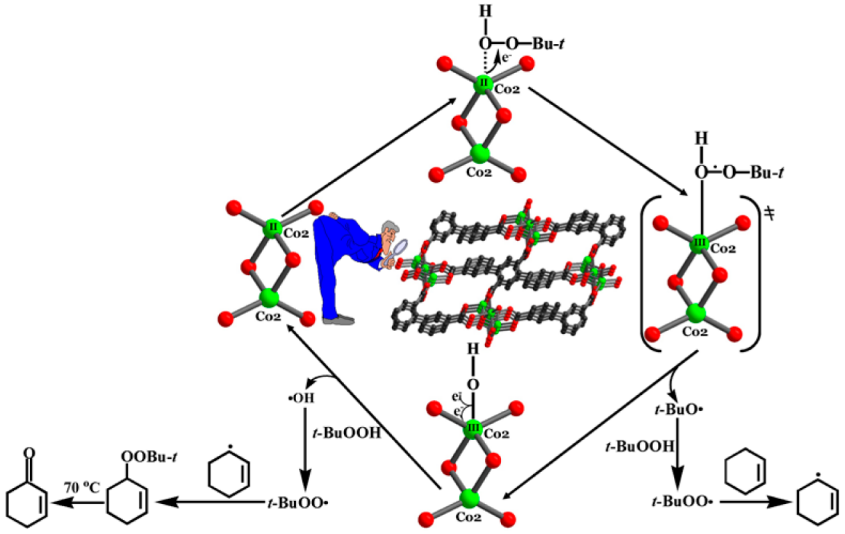

mation of 2-cyclohexen-1-one, *tert*-butyl-2-cyclohexenyl-1-peroxide, and cyclohexene oxide, which strongly indicates the dominant role of radical reactions in this oxidation.

On the basis of our results and previous mechanistic studies of cobalt catalysis,[7c,8,16] we put forward a plausible mechanism to elucidate the observed selectivity pattern (Scheme 2). In the initiation step, the flexibly assembled Lewis acid Co(II)2 ions in **1a** might be preferentially coordinated by an oxygen atom from *t*-BuOOH according to the soft and hard acids and bases theory. Electrons flow from the Co(II)2 atoms with unsaturated coordination environments to the peroxy bond of *t*-BuOOH, causing the weak O—O bond to break, and then *tert*-butoxy radicals (*t*-BuO·) might be created. The propagation steps: The resulting *t*-BuO· radical might abstract quickly a hydrogen atom from another *t*-BuOOH molecule. Consequently, a *t*-BuOO· radical and *t*-BuOH would be created. A majority of the *t*-BuOO· radicals might react directly with cyclohexene to yield a 3-cyclohexenyl radical. The resulting cobalt hydroxy species via fission of the Co—O bond could further form a ·OH radical, which likely reacts with another *t*-BuOOH molecule to produce a *t*-BuOO· radical. Then, the *t*-BuOO· radical might combine with a 3-cyclohexenyl radical to result in *tert*-butyl-2-cyclohexenyl-1-peroxide. However, the O—O bond of *tert*-butyl-2-cyclohexenyl-1-peroxide most likely thermally decomposes at 70 °C to give main product 2-cyclohexen-1-one, which strongly depends on the nature of the hydroperoxide.[1,8] Meanwhile, the cobalt hydroxy species could recover the initial catalyst **1a**, and the catalytic cycle starts over again.

CONCLUSION

In situ SCSC dehydration transformation of cobalt atoms from octahedron to unsaturated tetrahedron results in large changes in catalysis activity. Quite importantly, the dehydrated phase as true heterogeneous catalyst exhibits excellent catalytic activity and high selectivity toward 2-cyclohexene-1-one by increasing the surface area of **1a**. Meanwhile, under optimal conditions, dehydrated **1a** catalysts could be recycled at least three times without loss of the catalytic properties. The much lower energy of activation with dehydrated **1a** catalyst than hydrated **1** catalyst clearly suggested that coordinatively unsaturated Co^{II} sites in dehydrated **1a** have played a significant role in decreasing the energy of activation. Studies extending the scope of cyclic olefin that could be tolerated will be performed in the near future. Our finding will help one to understand the structure—activity relations of a catalyst, which might lead to commercial exploitation of the highly active Co-MOF catalysts toward formation of α,β unsaturated ketone.

ASSOCIATED CONTENT

Supporting Information

CCDC 1031319—1031320 in CIF format, crystal structural data for **1** and **1a**, experimental details, and additional figures and tables. The Supporting Information is available free of charge on the ACS Publications website at DOI: 10.1021/acs.inorgchem.5b00606.

AUTHOR INFORMATION

Corresponding Author

*E-mail: zhangxm@dns.sxnu.edu.cn (X.-M. Z.).

Notes

The authors declare no competing financial interest.

ACKNOWLEDGMENTS

Financial support from the 973 Program (2012CB821701), the Ministry of Education of China (Grant IRT1156), and NSFC (Grants 20925101 and 21401119) is greatly appreciated.

REFERENCES

(1) Sheldon, R. A.; Kochi, J. K. In *Metal-Catalyzed Oxidations of Organic Compounds*; Academic Press: London, 1981; Vol. 9.

(2) (a) Barf, G. A.; Sheldon, R. A. *J. Mol. Cata. A: Chem.* **1995**, *102*, 23—39. (b) Koola, J. D.; Kochi, J. K. *J. Org. Chem.* **1987**, *52*, 4545—4553. (c) Chavez, F. A.; Rowland, J. M.; Olmstead, M. M.; Mascharak, P. K. *J. Am. Chem. Soc.* **1998**, *120*, 9015—9027. (d) Groves, J. T.; Nemo, T. E. *J. Am. Chem. Soc.* **1983**, *105*, 5786—5791. (e) Groves, J. T.; Quinn, R. *J. Am. Chem. Soc.* **1985**, *107*, 5790—5792. (f) Meunier, B. E.; Guilmet, M.; Carvalho, E. De; Poilblanc, R. *J. Am. Chem. Soc.* **1984**, *106*, 6668—6676. (g) Nam, W.; Han, H. J.; Oh, S.-Y.; Lee, Y. J.; Choi, M.-H.; Han, S.-Y.; Kim, C.; Woo, S. K.; Shin, W. *J. Am. Chem. Soc.* **2000**, *122*, 8677—8684. (h) Tai, A. F.; Margerum, L. D.; Valentine, J. S. *J. Am. Chem. Soc.* **1986**, *108*, 5006—5008. (i) Traylor, T. G.; Miksztal, A. R. *J. Am. Chem. Soc.* **1989**, *111*, 7443—7448. (j) Agarwal, D. D.; Srivastava, S.; Chadha, P. *Polyhedron* **1990**, *9*, 487—489. (k) Rousselet, G.; Chassagnard, C.; Capdevielle, P.; Maumy, M.

DOI: 10.1021/acs.inorgchem.5b00606
Inorg. Chem. 2015, 54, 6312—6318

Tetrahedron Lett. **1996**, *37*, 8497−8500. (l) Sheldon, R. A. In *Fine Chemicals through Heterogeneous Catalysis*; Sheldon, R. A., van Bekkum, H., Eds.; Wiley-VCH: Weinheim, 2001; Vol. *9*. (m) Murphy, E. F.; Mallat, T.; Baiker, A. *Catal. Today* **2000**, *57*, 115−126. (n) Muzart, J. *Chem. Rev.* **1992**, *92*, 113−140.

(3) (a) Hao, Y.; Chong, Y.; Li, S.; Yang, H. *J. Phys. Chem. C* **2012**, *116*, 6512. (b) Yang, H. Q.; Wang, Y.; Qin, Y.; Chong, Y.; Yang, Q.; Li, G.; Zhang, L. *Green Chem.* **2011**, *13*, 1353−1361. (c) Yang, H. Q.; Ma, Z.; Wang, Y.; Wang, Y.; Fang, L. *Chem. Commun.* **2010**, *46*, 8659−8661.

(4) (a) Chui, S. S.; Lo, S. M.; Charmant, J. P.; Orpen, A. G.; Williams, I. D. *Science* **1999**, *283*, 1148−1150. (b) Horike, S.; Dinca, M.; Tamaki, K.; Long, J. R. *J. Am. Chem. Soc.* **2008**, *130*, 5854−5855. (c) Zhao, B.; Cheng, P.; Chen, X.-Y.; Cheng, C.; Shi, W.; Liao, D.-Z.; Yan, S.-P.; Jiang, Z.-H. *J. Am. Chem. Soc.* **2004**, *126*, 3012−3013. (d) Xiao, B.; Hou, H.-W.; Fan, Y.-T. *J. Organomet. Chem.* **2007**, *692*, 2014−2020.

(5) (a) Henschel, A.; Gedrich, K.; Kraehnert, R.; Kaskel, S. *Chem. Commun.* **2008**, 4192−4194. (b) Alaerts, L.; Séguin, E.; Poelman, H.; Thibault-Starzyk, F.; Jacobs, P. A.; De Vos, D. E. *Chem.—Eur. J.* **2006**, *12*, 7353−7363. (c) Schlichte, K.; Kratzke, T.; Kaskel, S. *Microporous Mesoporous Mater.* **2004**, *73*, 81−88. (d) Chen, Y.-Z.; Zhou, Y.-X.; Wang, H.; Lu, J.; Uchida, T.; Xu, Q.; Yu, S.-H.; Jiang, H.-L. *ACS Catal.* **2015**, *5*, 2062−2069.

(6) Cheng, X. N.; Zhang, W. X.; Lin, Y. Y.; Zheng, Y. Z.; Chen, X. M. *Adv. Mater.* **2007**, *19*, 1494−1498.

(7) (a) Tonigold, M.; Lu, Y.; Bredenkotter, B.; Rieger, B.; Bahnmuller, S.; Hitzbleck, J.; Langstein, G.; Volkmer, D. *Angew. Chem., Int. Ed.* **2009**, *48*, 7546−7550. (b) Shaabani, A.; Farhangi, E. *Appl. Catal., A* **2009**, *371*, 148−152. (c) Tonigold, M.; Lu, Y.; Mavrandonakis, A.; Puls, A.; Staudt, R.; Mollmer, J.; Sauer, J.; Volkmer, D. *Chem.—Eur. J.* **2011**, *17*, 8671−8695. (d) Chand, D. K.; Bharadwaj, P. K. *Inorg. Chem.* **1997**, *36*, 5658−5660. (e) Lu, Y.; Tonigold, M.; Bredenkötter, B.; Volkmer, D.; Hitzbleck, J.; Langstein, G. *Z. Anorg. Allg. Chem.* **2008**, *634*, 2411−2417.

(8) Skobelev, I. Y.; Sorokin, A. B.; Kovalenko, K. A.; Fedin, V. P.; Kholdeeva, O. A. *J. Catal.* **2013**, *298*, 61−69.

(9) Feng, D.; Jiang, H.-L.; Chen, Y.-P.; Gu, Z.-Y.; Wei, Z.; Zhou, H.-C. *Inorg. Chem.* **2013**, *52*, 12661−12667.

(10) Sheldrick, G. M. *SHELX-97: Program for X-ray Crystal Structure Solution and Refinement*; Göttingen University: Germany, 1997.

(11) (a) Zhang, X. M.; Hao, Z. M.; Zhang, W. X.; Chen, X. M. *Angew. Chem., Int. Ed.* **2007**, *46*, 3456−3459. (b) Li, X. J.; Wang, X. Y.; Gao, S.; Cao, Y. *Inorg. Chem.* **2006**, *45*, 1508−1516. (c) Livage, C.; Férey, G. *Chem. Mater.* **1999**, *11*, 1546−1550. (d) Huang, Z. L.; Drillon, M.; Masciocchi, N.; Sironi, A.; Zhao, J. T.; Rabu, P.; Panissod, P. *Chem. Mater.* **2000**, *12*, 2805−2812. (e) Kumagai, H.; Kepert, C. J.; Kurmoo, M. *Inorg. Chem.* **2002**, *41*, 3410−3422. (f) Yang, F.; Li, B. Y.; Xu, W.; Li, G. H.; Zhou, Q.; Hua, J.; Shi, Z.; Feng, S. H. *Inorg. Chem.* **2012**, *51*, 6813−6820.

(12) van der Sluis, P.; Spek, A. L. *Acta Crystallogr., Sect. A* **1990**, *46*, 194−201.

(13) (a) Galli, S.; Masciocchi, N.; Tagliabue, G.; Sironi, A.; Navarro, J. A. R.; Salas, J. M.; Mendez-Liñan, L.; Domingo, M.; Perez-Mendoza, M.; Barea, E. *Chem.—Eur. J.* **2008**, *14*, 9890−9901. (b) Poul, L.; Jouini, N.; Fiévet, F. *Chem. Mater.* **2000**, *12*, 3123−3132. (c) Song, W.-C.; Li, J.-R.; Song, P.-C.; Tao, Y.; Yu, Q.; Tong, X.-L.; Bu, X.-H. *Inorg. Chem.* **2009**, *48*, 3792−3799. (d) Ma, R.; Liu, Z.; Takada, K.; Fukuda, K.; Ebina, Y.; Bando, Y.; Sasaki, T. *Inorg. Chem.* **2006**, *45*, 3964−3969. (e) Zeng, M. H.; Wang, B.; Wang, X. Y.; Zhang, W. X.; Chen, X. M.; Gao, S. *Inorg. Chem.* **2006**, *45*, 7069−7076.

(14) (a) Tulip, P. R.; Bates, S. P. *J. Phys. Chem. C* **2009**, *113*, 19310−19316. (b) Gagnon, K. J.; Beavers, C. M.; Clearfield, A. *J. Am. Chem. Soc.* **2013**, *135*, 1252−1255. (c) Biradha, K.; Hongo, Y.; Fujita, M. *Angew. Chem., Int. Ed.* **2002**, *41*, 3395−3398. (d) Zhao, N.; Sun, F.; He, H.; Jia, J.; Zhu, G. S. *Cryst. Growth Des.* **2014**, *14*, 1738−1743. (e) Aijaz, A.; Lama, P.; Bharadwaj, P. K. *Inorg. Chem.* **2010**, *49*, 5883−5889. (f) Jayashree, R. S.; Vishnu Kamath, P. *J. Mater. Chem.* **1999**, *9*, 961−963. (g) Abraham, B. D.; Sono, M.; Boutaud, O.; Shriner, A.; Dawson, J. H.; Brash, A. R.; Gaffney, B. J. *Biochemistry* **2001**, *40*, 2251−2259.

(15) (a) Bravo, A.; Bjørsvik, H.-R.; Fontana, F.; Liguori, L.; Minisci, F. *J. Org. Chem.* **1997**, *62*, 3849−3857. (b) Lu, Y.; Tonigold, M.; Bredenkötter, B.; Volkmer, D.; Hitzbleck, J.; Langstein, G. *Z. Anorg. Allg. Chem.* **2008**, *634*, 2411−2417.

(16) (a) Nam, W.; Kim, H. J.; Kim, S. H.; Ho, R. Y. N.; Valentine, J. S. *Inorg. Chem.* **1996**, *35*, 1045−1049. (b) Cao, Y.-H.; Yu, H.; Peng, F.; Wang, H.-J. *ACS Catal.* **2014**, *4*, 1617−1625.

DOI: 10.1021/acs.inorgchem.5b00606
Inorg. Chem. 2015, 54, 6312−6318